Contagion, Migration and Misallocation in a Pandemic[*]

Ke Tang[†]
Tsinghua University

Danxia Xie[‡]
Tsinghua University

Longtian Zhang[§]
Central University of Finance and Economics

Version: 1.0

Date: December 26, 2021

Abstract

We present a multi-city migration model to study the endogenous choices of migration during a pandemic and to evaluate various policy alternatives as well. Analytical solutions are provided under the two situations respectively: laissez-faire equilibrium and social optimum. We find that migration rates diverge under these two situations, especially for the infected people. We also provide a new cross-country empirical fact that countries with higher COVID-19 mortality disparity across sub-regions tend to have lower nationwide mortality rates. This new fact is inconsistent with the prediction of the traditional misallocation literature, nevertheless is aligned with our theoretical model, which can be seen as an extension of the misallocation framework with cross-region contagion and externality. In addition, through numerical analyses we observe that the total social welfare can be increased by up to 2% in two-week time span with better policies. This research can shed light on policy design under pandemic threat and also help to enrich the misallocation literature.

Keywords: SIR Model, Migration, Misallocation, Hospital Resource, Pandemic
JEL Code: I18, E61

---

[*] Tang and Xie are grateful for the financial support from the National Natural Science Foundation of China (Grant No. 71973075, 71973076). The contents of this publication are solely the responsibility of the authors.

[†] Institute of Economics, Tsinghua University, Beijing, China 100084. Email: ketang@tsinghua.edu.cn.

[‡] (Corresponding author) Institute of Economics, Tsinghua University, Beijing, China 100084. Email: xiedanxia@tsinghua.edu.cn.

[§] School of International Trade and Economics, Central University of Finance and Economics, Beijing, China 102206. Email: zhanglongtian@cufe.edu.cn.

1 Introduction

Since its discovery in December 2019, COVID-19 has unexpectedly become one of the most serious and widespread pandemics. By the end of 2021, 280 million infected and 5.4 million deaths from this disease had been confirmed worldwide. The academic literature related to this disease has burgeoned after the outbreak, giving rise to different lines of research. Among these, we can highlight the one related to the lockdown policy and the problems arising from social distancing requirements (e.g., Acemoglu et al., 2020; Farboodi et al., 2020; Jones et al., 2021). However, most of these studies refer to the policies carried out within a city, while the restrictions on movements between regions and the agents' decisions as a result of these restrictions have not been sufficiently analyzed.[1] In addition, the efficiency in the use and allocation of hospital resources across regions has also been under-studied in the economic literature related to the pandemic. Our paper attempts to fill in this gap.

If there is no severe misallocation, the death rate for COVID-19 should be approximately the same across regions and close to the national average, as this rate can be seen as a rough measure of productivity of the health sector in each region. Nevertheless, a simple empirical analysis contradicts this conclusion, as illustrated in Table 1. From the table, we see that Hubei province where Wuhan is located, has a death rate which is higher than the national average level, and much higher than other major cities of China. The uneven distribution of medical resources across cities and areas could induce large-scale migrations that would exacerbate the spread of the virus. On the other hand, these migrations could help to equalize the amount of hospital resources per capita through the different areas, mitigating the resource misallocation problem. Therefore, there exists some kind of trade-off in terms of migration control from the policy perspective. For a country like China, although misallocation exists (see Table 1) due to migration control policies, the total number of infections nationwide is minimized with aggregate social welfare enhancing. In contrast, the United States has experienced much higher total loss of lives despite achieving a lower national mortality rate. These facts are inconsistent with the predictions of the traditional misallocation literature, nevertheless is aligned with our model presented in this paper, which can be seen as an extension of the misallocation framework with cross-region contagion and externality. Specifically, we develop a new theoretical model considering resource endowment, endogenous migration choices, as well as misallocation and reallocation as policy instruments. In addition, and unlike most of the papers in the related literature, we find closed-form solutions of our model, which can facilitate the understanding of pandemic economics

[1] Some papers have been dedicated to multi-city models (e.g., Bisin and Moro, 2020; Fajgelbaum et al., 2020), but focusing only on the network effects, without considering personal decisions.

and policy design.

Our model emphasizes the endogenous migration decisions of different population groups across cities or regions during a pandemic, which has not been paid sufficient attention in related research.[2] There are three important factors that an agent considers when making migration decisions: (1) the relative medical resources of cities as aforementioned; (2) the probability of being infected in a particular city; (3) migration costs. An uninfected agent might want to move to a city with less infected people, while an infected patient would intend to migrate to a city with better medical treatment. Moreover, an agent will also take into account the choices of all other agents when making his/her own decisions. If an uninfected agent expects more infected patients to move to a city, he/she will try to avoid entering that city in order to reduce his/her risk of contagion. This will eventually lead to a rational expectation equilibrium where every agent will have correctly anticipated all the other agents' real actions.

Related literature—One of the most important tools to help researchers and policy makers understand the trend of a pandemic is the classical SIR model first proposed by Kermack et al. (1927). In the simplest version of the model, agents are divided into three types: susceptible, infected and recovered. Susceptible agents meet infected ones and have a probability of getting infected, and the infected agents recover from the disease at a certain rate. The changes in the number of each type of agents are described by several differential equations. Some other models have extended this framework in order to make it more meaningful (e.g., Chowell et al., 2003; Stehlé et al., 2011). After the pandemic outbreak, many new papers appeared that added economic trade-offs into the traditional SIR and other SIR-like models to study corresponding policy implications. In general terms, we can divide these papers into two categories, according to the main topic they address: the estimation of the economic impact and the optimization of lockdown policies. Regarding the former, Fernàndez-Villaverde and Jones (2020), Hall et al. (2020), and Guerrieri et al. (2020) estimated the negative effects of this pandemic on the economy of the U.S. and other countries in the world; Eichenbaum et al. (2021) proposed a macroeconomic model combining testing and quarantining; and Fang et al. (2020) estimated the effect of traveling restrictions in China during the pandemic, and provided some important insights to our paper on the migration of population. On the other hand, lockdown policy is another important topic which has attracted many researchers to work on it. Alvarez et al. (2021) opened a new line of research on this topic, which was continued by other important papers, by proposing a framework that combines the SIR model with an economic optimization problem. Finally, we should mention that it is not the first time that the multi-city SIR-like model used in our paper is applied in research (see, for example,

[2]Studies on endogenous decisions among different health states are not frequently seen in literature. One example is Chan et al. (2016), which provides an theoretical model describing the influence of HAART, a breakthrough of HIV treatment, on the corresponding precaution behaviors.

Bobashev et al., 2011; Chinazzi et al., 2020), but these papers do not include, unlike ours, the endogenous decisions of agents, which constitutes an important contribution from the economic point of view.

Our paper studies the misallocation of hospital resources during a pandemic, and the migration decisions made to mitigate this inefficiency. Since the appearance of Hsieh and Klenow (2009), misallocation has become a hot topic, giving rise to a growing literature that extends the misallocation of productivity that they study to different aspects of our lives (e.g., Dower and Markevich, 2018; Hsieh et al., 2019; Tombe and Zhu, 2019). In these papers, misallocation is always interpreted as an undesirable phenomenon. However, in the specific setting provided in our paper, misallocation coming from the uneven hospital load among different cities shows a positive effect in reducing the total loss caused by the pandemic. The reason lies in the contagion risk associated with the free movement of the agents, and misallocation becomes desirable when the harm caused by this kind of externality increases considerably.

The remainder of this paper is organized as follows. Section 2 provides the general settings of our model, including some details on agents' decisions and the aggregate moving equations. Section 3 gives the explicit solutions of the migration decisions under two different situations. Section 4 provides some numerical results on the impact of allocation of hospital resources, welfare analysis, and some numerical examples to show the special misallocation in this paper. Finally, Section 5 concludes.

2 The Model

In this section, we introduce the general settings of our model. First, we provide the processes related to migration decisions. Next, we propose the aggregate moving equations of an n-city SIR-like model, and explain the meaning of some time-variant parameters.

2.1 Agents

Agents only care about their health states and consumption, following the model of Grossman (1972). Formally, for a single agent, we set the utility function in the form,

$$u(c_t; h_t) = c_t + \phi h_t,$$

where c_t is the consumption level of the agent, h_t is the utility from the health state, and ϕ is the weight of health state in the utility function. At the beginning of every period, agents are informed of the numbers of infected, recovered and dead people in all the cities in the last period, and they know all the relating parameters of the epidemic model. Thus, they can influence the expected health state of the following period by setting their own optimal migration rates from the city they live in to all the other cities.

Every period, each agent receives w units of endowment, which can be distributed between consumption and fees paid to change his/her own migration rates. Thus, the budget constraint is

$$c_t + f_t = w.$$

The utility of health state h_t takes the following values. If the agent is healthy, $h_t = 1$. If the agent becomes infected, $0 < h_t = u_I < 1$. When an agent is recovered from the disease, the utility will return to the same level as those susceptible ones. However, if an agent is dead, there will be a high disutility value, i.e., $h_t = u_D \ll 0$.

The migration rates are determined as follows. Consider n cities, with populations N_1, N_2,..., N_n, where n is finite and no smaller than 2. Agents can move from one city to another. In peacetime, we expect that the populations of these cities remain constant. That is, there exist natural migration rates which satisfy the following equations simultaneously.[3] For any $i = 1, 2, ..., n$, we have

$$N_i \sum_{j=1, j\neq i}^{n} \bar{\eta}_{ij} = \sum_{j=1, j\neq i}^{n} \bar{\eta}_{ji} N_j,$$

where $\bar{\eta}_{ij}$ is the natural migration rate from city i to city j. When a pandemic comes, agents pay to make their own migration rates deviate from the corresponding natural level. Formally, let η_{ij}, $i, j = 1, 2, ..., n$, $i \neq j$ be the actual migration rates from city i to city j. Then, the fee an agent who lives in city i has to pay to achieve these rates is set as

$$f_i = \sum_{j=1, j\neq i}^{n} k_{ij} (\eta_{ij} - \bar{\eta}_{ij})^2. \tag{1}$$

One should note that, for a single agent, the migration rates he/she chooses can be viewed as the probabilities of being in a certain city in the next period, and the agent arranges these probabilities in order to maximize his/her expected utility. This probabilistic interpretation can be justified by considering the agent of our model as an "average" person. Obviously, if an agent does not want to move at all, he/she should pay $\sum_{j=1, j\neq i}^{n} k_{ij} \bar{\eta}_{ij}^2$ to make all the corresponding probabilities equal to zero.

[3] Natural migration rate defined here is just a shortcut of our model. In models like Tombe and Zhu (2019), researchers usually add an idiosyncratic preference term for different cities in the agents' utility functions to describe the migrating behavior. However, we think this preference is dominated by the concern of health states when a pandemic comes. As a result, we ignore this in our utility function. Also, we assume that the fees paid to deviate from the natural migration rate dominate the fees of migrating in peacetime (the fees to achieve natural migration rates), and come to the setting in (1).

2.2 Aggregate Moving Equations

When a pandemic comes, agents in each city are divided into four types: susceptible (S), infected (I), recovered (R) and dead (D). At the beginning to period t, the numbers of all types of agents are $S_i(t)$, $I_i(t)$, $R_i(t)$ and $D_i(t)$, $i = 1, 2, ..., n$. In order to maximize their expected utilities, agents decide (or social planner decide when we derive the optimal policy) which cities to live in this period. After the migrations, numbers of all types of agents become $S'_i(t)$, $I'_i(t)$, $R'_i(t)$ and $D'_i(t)$, $i = 1, 2, ..., n$, according to

$$U'_i(t) = \left(1 - \sum_{j=1,j\neq i}^{n} \eta_{U,ij}\right) U_i(t) + \sum_{j=1,j\neq i}^{n} \eta_{U,ji} U_j(t), \quad i = 1, 2, ..., n. \tag{2}$$

Here, we define the actual number of these types of agents after migration at the current period as $U'_1(t)$, $U'_2(t)$,..., $U'_n(t)$, $U = S, I, R$ (assume that dead agents do not migrate). These variables can be viewed as transitional states at period t. Then, agents begin to commute between the cities, or go to hospitals for treatments. During this process, susceptible agents may have the possibility to meet an infected one and get infected, or infected agents being treated in hospitals may be cured or die. At the end of this period, numbers of all types of agents become $S_i(t + 1)$, $I_i(t + 1)$, $R_i(t + 1)$ and $D_i(t + 1)$, $i = 1, 2, ..., n$, according to the equations shown from (4) to (7). Then, a new period begins. To make the above illustrations more explicit, we show the timeline of the model in Figure 1.

Based on the transitional states defined in (2), we define the total population of city i after migration as

$$N'_i(t) = S'_i(t) + I'_i(t) + R'_i(t). \tag{3}$$

Then, the aggregate moving equations of agents in city i, $i = 1, 2, ..., n$, are:

$$S_i(t + 1) = S_i(t) - \frac{\beta}{N'_i(t)} S'_i(t) I'_i(t) - S_i(t) \sum_{j=1,j\neq i}^{n} \eta_{S,ij} + \sum_{j=1,j\neq i}^{n} \eta_{S,ji} S_j(t), \tag{4}$$

$$I_i(t + 1) = I_i(t) + \frac{\beta}{N'_i(t)} S'_i(t) I'_i(t) - [\gamma_i(t) + \lambda_i(t)] I'_i(t) - I_i(t) \sum_{j=1,j\neq i}^{n} \eta_{I,ij} + \sum_{j=1,j\neq i}^{n} \eta_{I,ji} I_j(t), \tag{5}$$

$$R_i(t + 1) = R_i(t) + \gamma_i(t) I'_i(t) - R_i(t) \sum_{j=1,j\neq i}^{n} \eta_{R,ij} + \sum_{j=1,j\neq i}^{n} \eta_{R,ji} R_j(t), \tag{6}$$

$$D_i(t + 1) = D_i(t) + \lambda_i(t) I'_i(t). \tag{7}$$

In these equations, β is the conditional transmission probability of the disease. The migration rates of different types of agents in different cities can be various, which will be further discussed below.

In every period, susceptible agents may be exposed to the virus and have a chance (with probability β) to get infected. Once an agent becomes infected, in every period, he/she has a probability of γ to become a recovered one, and a probability of λ to die. Once an agent recovers, he/she will never get infected again. However, when an agent dies, he/she will bear a high level of disutility and no longer be able to move again.

The recovering rate $\gamma_i(t)$ and the death rate $\lambda_i(t)$ need to be explained in more details. In every period, the probability of recovering from sickness in city i is

$$\gamma_i(t) = \bar{\gamma} - \kappa_1 \left(\frac{I_i'(t)}{H_i} \right),$$

where $I_i'(t)$ is obtained in (2). H_i represents the abundance of hospital resources in city i, which is viewed as a constant in the model. Finally, $\bar{\gamma}$ and κ_1 are parameters in the determining equation of recovering rate, with $\bar{\gamma}, \kappa_1 > 0$. Similarly, we set the probability of dying from the disease in every period as

$$\lambda_i(t) = \bar{\lambda} + \kappa_2 \left(\frac{I_i'(t)}{H_i} \right),$$

where $\bar{\lambda}$ and κ_2 are parameters in the determining equation, with $\bar{\lambda}, \kappa_2 > 0$, and the meaning of $I_i'(t)$ is the same as in (2). It is important to note that the equations determining the recovery rate and the death rate are only applicable when the ratios of infected agents and hospital resources are within a certain range because these equations are linear, and $\gamma_i(t)$, $\lambda_i(t)$ must belong to $[0, 1]$.

One should also note that, since recovered agents will never get infected again, they will not pay any more to deviate from the natural level of migration. In other words, the migration rates of recovered agents in all the cities always equal to the natural level, i.e., $\eta_{R,ij} = \bar{\eta}_{ij}$, $i, j = 1, 2, ..., n$, $i \neq j$. Then, we set $\tilde{\eta}_{U,ij}$, $U = S, I$, $i, j = 1, 2, ..., n$, $i \neq j$, as the migration rates determined independently by the corresponding types of agents. Here, we use tildes to distinguish migration decisions made by agents themselves from the aggregate migration rates. $p_{i,t}$, $q_{i,t}$ and $r_{i,t}$ represent the infectious rate, the recovering rate and the death rate in city i, respectively. Considering migration, these rates can be written as follows.

$$p_{i,t} = \beta \frac{I_i'(t)}{N_i'(t)}, \quad q_{i,t} = \gamma_i(t) = \bar{\gamma} - \kappa_1 \left(\frac{I_i'(t)}{H_i} \right), \quad r_{i,t} = \lambda_i(t) = \bar{\lambda} + \kappa_2 \left(\frac{I_i'(t)}{H_i} \right).$$

For the sake of tractability, we assume that the changes of total populations in each city between two neighboring periods are very trivial and thus (3) can be simplified in the approximated form

$$N_i'(t) \approx N_i(0) - D_i(t).$$

Based on the settings above, and given the aggregate numbers of all types of agents in the last period, an agent can expect his/her expected health state in the current period according to a transition matrix, which is shown in Table 2, and then make decisions on different migration rates to different cities in that period.

3 Migration Decisions

In this section, we obtain the migration decisions between two neighboring periods given the number of all types of agents in the last period. The current expected utility of an agent in city i now if he/she was a susceptible one in the last period is

$$\begin{aligned}
&E[u(c_t; h_t, h_{t-1} = \text{susceptible}, i)] \\
=&w - f(\tilde{\eta}_{S,ij}; j \neq i) + \phi \Bigg[\left(1 - \sum_{j\neq i} \tilde{\eta}_{S,ij}\right)(1 - p_{i,t}) + u_I \left(1 - \sum_{j\neq i} \tilde{\eta}_{S,ij}\right) p_{i,t} + \\
&\sum_{j\neq i} \left(\tilde{\eta}_{S,ij}(1 - p_{j,t}) + \tilde{\eta}_{S,ij} p_{j,t} u_I\right) \Bigg].
\end{aligned}$$

Similarly, the current expected utility for an agent that was infected in the last period can be derived as

$$\begin{aligned}
&E[u(c_t; h_t, h_{t-1} = \text{infected}, i)] \\
=&w - f(\tilde{\eta}_{I,ij}; j \neq i) + \phi \Bigg[\left(1 - \sum_{j\neq i} \tilde{\eta}_{I,ij}\right)(1 - q_{i,t} - r_{i,t}) u_I + \left(1 - \sum_{j\neq i} \tilde{\eta}_{I,ij}\right) q_{i,t} \\
&+ \left(1 - \sum_{j\neq i} \tilde{\eta}_{I,ij}\right) r_{i,t} u_D + \sum_{j\neq i} (\tilde{\eta}_{I,ij}(1 - q_{j,t} - r_{j,t}) u_I + \tilde{\eta}_{I,ij} q_{j,t} + \tilde{\eta}_{I,ij} r_{j,t} u_D) \Bigg].
\end{aligned}$$

In this paper, we mainly compare the migration decisions made by individuals (laissez-faire equilibrium) and by a benevolent government which aims to maximize the total utility of all the agents in all the cities (optimal policy). These two situations will be discussed below.

3.1 Laissez-Faire Equilibrium

We first consider the laissez-faire equilibrium in which agents make decisions independently. This situation can be viewed as a pandemic with no government intervening migrations. The derivation of this equilibrium is shown in Appendix A. Denote the solutions of the migration rates as

$$\boldsymbol{\eta}_L = [\eta_{S,12}, \eta_{S,21}, ..., \eta_{S,(n-1)n}, \eta_{S,n(n-1)}, \eta_{I,12}, \eta_{I,21}, ..., \eta_{I,(n-1)n}, \eta_{I,n(n-1)}]',$$

which is a $2n(n-1) \times 1$ vector, and the subscript "L" stands for the variables in laissez-faire equilibrium. Then, given the total number of different types of agents I_i, D_i, $i = 1, 2, ..., n$, in the last period, in laissez-faire equilibrium, these migration rates can be obtained from the system of linear equations

$$\boldsymbol{A}_L \boldsymbol{\eta}_L = \boldsymbol{B}_L, \tag{8}$$

where $\boldsymbol{A}_L$ is a $2n(n-1) \times 2n(n-1)$ matrix, and $\boldsymbol{B}_L$ is a $2n(n-1) \times 1$ vector. Let $A_{L,(U,ij),(U',kl)}$ be the element of matrix $\boldsymbol{A}_L$ which corresponds to the row of $\eta_{L,U,ij}$ and the column of $\eta_{L,U',kl}$, and let $B_{L,(U,ij)}$ be the element of vector $\boldsymbol{B}_L$ which corresponds to $\eta_{L,U,ij}$, $U = S, I$. By setting down the matrix $\boldsymbol{A}_L$ and the vector $\boldsymbol{B}_L$, the migration rates can be obtained as

$$\boldsymbol{\eta}_L = \boldsymbol{A}_L^{-1} \boldsymbol{B}_L.$$

As for the elements in matrix $\boldsymbol{A}_L$ and vector $\boldsymbol{B}_L$, we have the following proposition.

Proposition 3.1. *In the laissez-faire equilibrium, the elements of matrix $\boldsymbol{A}_L$ and vector $\boldsymbol{B}_L$ are shown in Table 3. Specifically, matrix $\boldsymbol{A}_L$ can be divided into the following four blocks:*

$$\boldsymbol{A}_L = \begin{bmatrix} \boldsymbol{A}_{L,SS} & \boldsymbol{A}_{L,SI} \\ \boldsymbol{A}_{L,IS} & \boldsymbol{A}_{L,II} \end{bmatrix}.$$

These four block matrices are all $n(n-1) \times n(n-1)$ matrices, and they have the following properties:

1. *$\boldsymbol{A}_{L,SS}$ is an $n(n-1) \times n(n-1)$ identity matrix.*
2. *$\boldsymbol{A}_{L,IS}$ is an $n(n-1) \times n(n-1)$ null matrix.*
3. *$\boldsymbol{A}_{L,SI}$ and $\boldsymbol{A}_{L,II}$ are non-singular matrices.*

Since $\boldsymbol{A}_L$ is non-singular and $\boldsymbol{B}_L$ is non-zero, we can uniquely determine the migration decisions of the agents.

In the table, constants C_S and C_I are shown as follows:

$$C_S = \frac{\beta\phi}{2}(1 - u_I) \tag{9}$$

and

$$C_I = \frac{\phi}{2}\left[\kappa_1(1 - u_I) + \kappa_2(u_I - u_D)\right]. \tag{10}$$

Here, I_i, D_i, $i = 1, 2, ..., n$ represent the number of different types of agents in the last period, and N_i, $i = 1, 2, ..., n$ are the initial populations of the n cities.

3.2 Optimal Policy

In this section, we consider a social planner who decides the optimal migration rates taking into account the welfare of the whole population. This can be thought as the most ideal situation during a pandemic, with collective actions led by the government. Formally, the social planner maximizes the following problem,

$$E[U(c_{1,t}, ..., c_{j,t}, ...; h_{1,t}, ..., h_{j,t}, ...)|\mathscr{F}_{t-1}] = \sum_{j=1}^{\sum_{k=1}^{n} N_k(0)} c_{j,t} + \phi E[h_{j,t}|\mathscr{F}_{t-1}],$$

where $\mathscr{F}_{t-1} = \{h_{1,t-1}, ..., h_{j,t-1}, ...\}$ represents the information set known in the last period, i.e., the number of all types of agents. Then, the above problem can be further written as

$$\begin{aligned}
&E[U(c_{1,t}, ..., c_{j,t}, ...; h_{1,t}, ..., h_{j,t}, ...)|\mathscr{F}_{t-1}] \\
=&\sum_{i=1}^{n} S_i \left\{ w - f(\eta^*_{S,ij}; j \neq i) + \phi \left[\left(1 - \sum_{j\neq i} \eta^*_{S,ij}\right)(1 - p_{i,t}) + u_I \left(1 - \sum_{j\neq i} \eta^*_{S,ij}\right) p_{i,t} + \right.\right. \\
&\left.\left. \sum_{j\neq i} \left(\eta^*_{S,ij}(1 - p_{j,t}) + \eta^*_{S,ij} p_{j,t} u_I\right) \right] \right\} + \sum_{i=1}^{n} I_i \left\{ w - f(\eta^*_{I,ij}; j \neq i) + \phi \left[\left(1 - \sum_{j\neq i} \eta^*_{I,ij}\right) \right.\right. \\
&(1 - q_{i,t} - r_{i,t}) u_I + \left(1 - \sum_{j\neq i} \eta^*_{I,ij}\right) q_{i,t} + \left(1 - \sum_{j\neq i} \eta^*_{I,ij}\right) r_{i,t} u_D + \sum_{j\neq i} (\eta^*_{I,ij}(1 - q_{j,t} - \\
&\left.\left. r_{j,t}) u_I + \eta^*_{I,ij} q_{j,t} + \eta^*_{I,ij} r_{j,t} u_D) \right] \right\} + \sum_{i=1}^{n} \left[R_i(w + \phi) + D_i(w + \phi u_D)\right].
\end{aligned} \tag{11}$$

Unlike the laissez-faire equilibrium, now the migration rates $\eta^*_{S,ij}$ and $\eta^*_{I,ij}$, $i, j = 1, 2, ..., n$, $i \neq j$, are determined simultaneously. It is also important to note that, in this case, $p_{i,t}$, $q_{i,t}$, $r_{i,t}$, $i = 1, 2, ..., n$ are functions relating to some migration rates of infected agents, so the government can also determine these rates by influencing the migration rates. The derivation of this optimal policy is shown in Appendix B. In the following, we add the subscript "O" to represent the variables in the optimal policy. The system of linear equations that determines the social optimal migration rates can also be defined in a similar way to that in the laissez-faire equilibrium, i.e.,

$$\boldsymbol{A}_O \boldsymbol{\eta}_O = \boldsymbol{B}_O. \tag{12}$$

As for the elements of $\boldsymbol{A}_O$ and $\boldsymbol{B}_O$, we have the following proposition.

Proposition 3.2. *In the optimal policy, the elements of matrix $\boldsymbol{A}_O$ and vector $\boldsymbol{B}_O$ are shown in Table 3. Specifically, matrix $\boldsymbol{A}_O$ can be divided into the following four blocks:*

$$\boldsymbol{A}_O = \begin{bmatrix} \boldsymbol{A}_{O,SS} & \boldsymbol{A}_{O,SI} \\ \boldsymbol{A}_{O,IS} & \boldsymbol{A}_{O,II} \end{bmatrix}.$$

These four block matrices are all $n(n-1) \times n(n-1)$ matrices, and they have the following properties:

1. *$\boldsymbol{A}_{O,SS}$ is an $n(n-1) \times n(n-1)$ identity matrix.*
2. *$\boldsymbol{A}_{O,SI}$, $\boldsymbol{A}_{O,IS}$ and $\boldsymbol{A}_{O,II}$ are all non-singular matrices.*
3. *$\boldsymbol{A}_{O,SI} = \boldsymbol{A}_{L,SI}$ but $\boldsymbol{A}_{O,II} \neq \boldsymbol{A}_{L,II}$.*

Since $\boldsymbol{A}_O$ is non-singular and $\boldsymbol{B}_O$ is non-zero, we can uniquely determine the migration decisions of the agents.

In this paper, we mainly concern about the influence of change in hospital resources allocation to the migration decisions. However, in this n-city model, it is not feasible to obtain an analytical solution for this effect. A simplified model with two cities is presented in Appendix D to obtain some primary conclusions, but we find it incomplete to fully describe the migration behavior of agents. As a result, we turn to numerical analysis in the next section to further study this problem, as well as other issues like welfare analysis and misallocation problem.

4 Numerical Examples

4.1 Methodology and Calibration

In this section, we come to some important conclusions based on the solutions we derive in the previous section. For simplicity, instead of the n-city model proposed in the previous section, we consider a model with three cities since it is good enough to show the main migration trends during a pandemic. The three cities we study here have the same population N, and the same natural migration rates $\bar{\eta}$ as well as their corresponding fee rates k between each other. The differences between cities are the following. First, the numbers of infected agents are different: City 1 has the largest number, city 2 has a medium number, and the number of infected agents in city 3 is nearly zero. Second, hospital resources allocated in these three cities are different: City 2 has the most abundant resources, city 1 has a medium level of resources but without satisfying the needs of its infected agents, and city 3 has few resources. We can image that these three cities are like Wuhan (the epidemic focus of the pandemic), Beijing (a big city that has abundant hospital resources) and a remote and underdeveloped city, respectively.

Before analysing, we should determine the parameters of the model. We use the method from Yang et al. (2020) to estimate the conditional transmission probability β, which is approximately 0.4. The determining parameters of the recovering rate and the death rate are set to ensure that the two rates are close to the data in China, where I/H approximates 1, which means hospitals are fully loaded. Formally, these parameters are set as: $\bar{\gamma} = 0.04$, $\bar{\lambda} = 0.0008$, $\kappa_1 = 0.01$ and $\kappa_2 = 0.0005$. Furthermore, since our model is just a two-period one, in order to match data, the time span of the parameters should be extended to a larger scale, e.g., a two-week scale. Thus, in practice, we take $\beta' = 5.6$ and other parameters are also re-scaled similarly. After re-scaling, these parameters become $\bar{\gamma}' = 0.56$, $\bar{\lambda}' = 0.0112$, $\kappa_1' = 0.14$ and $\kappa_2' = 0.007$. Finally, the population of each of the three cities are all set as $N = 10,000$, with city 1 being allocated 1,000 units of hospital resources (H_1), while city 2 and city 3 are allocated 3,000 and 100 units (H_2 and H_3), respectively. Each agent receives 1 unit of endowment w in a period, and the weight of health state in utility function are set as $\phi = 100$. When the agents get sick, their health state utility becomes $u_I = 0.5$ and when they are dead, it becomes $u_D = -10$. On the other hand, the natural migration rates between cities are $\bar{\eta} = 0.1$, and the corresponding fee rates all set as $k = 100$ to satisfy that an agent can use his/her entire endowment to make the migration rates zero. The fee rates should also be re-scaled as $k' = 1,400$, while the natural migration rates remain unchanged since they are possibilities and are limited within the range $[0, 1]$.

4.2 Allocations of Hospital Resources

In this subsection we will mainly focus on the problem of allocation of hospital resources during a pandemic. Infected agents compare the medical care level of different cities and choose to put larger possibility of migration on the one with higher recovering rate and lower death rate. At the same time, susceptible agents care about which city has the largest risk of getting infected, and given the decision patterns of infected agents, they choose to move to cities with less infected ones living in. We move some hospital resources from city 2 to city 1 to study the influence of resource reallocation to the migration decisions, which are shown in Figure 2.

Remind that the natural migration rates between each of the cities are all set as $\bar{\eta} = 0.1$. Thus, agents of a certain type choose to move out of a city to another one if the actual migration rate is larger than 0.1, while they choose not to move to the destination city if it is smaller than 0.1. As a result, we can observe from Figure 2 that, all susceptible agents choose to move to city 3, while infected agents decide to move to the city with more abundant resources. Moreover, by comparing the solid line (laissez-faire equilibrium) and the dash line (optimal policy), we can draw the following conclusion: When agents want to move out of a city, migration rates determined in optimal policy are always higher; when agents do not want to move out, the rates in optimal policy are always lower. In other words, migrating decisions made by social planner are always are more sensitive.

Some important panels in the figure should also be mentioned. By comparing the panels correspond to $\eta_{S,12}$ and $\eta_{S,13}$, we can conclude that susceptible agents in city 1 are more inclined to move to city 3 than to city 2, which shows that although city 3 has less hospital resources, susceptible agents care more about the possibility of getting infected than the medical care level. It is also interesting to look into the panel corresponding to $\eta_{I,12}$. In this panel, although both lines decrease as the hospital resources allocated in city 1 increases, in laissez-faire equilibrium, infected agents in city 1 tend to move out of the city in order to get better treatments; while in optimal policy, the social planner tend to prevent these agents from moving out, with the consideration of reducing the risk of infecting agents in other cities. We should note that under the optimal policy, agents in city 1 will face more crowded hospitals and poorer medical treatments due to the large number of patients falling ill. However, regarding the whole society, their sacrifice will lead to less infections and improvements in total social welfare. Some measures can be taken to mitigate this suffering, e.g., the reinforcement of hospital resources from other cities. This is what the Chinese government did during the most serious months in the pandemic, and the result is without doubt very effective. In the next section, we will further discuss this problem through welfare analysis.

4.3 Welfare Analysis

In this subsection, we conduct the welfare analysis to further illustrate the importance of collective actions in a pandemic. The definition of total social welfare are base on equation (11), and the results in laissez-fair equilibrium (LF) and optimal policy (OP) are both calculated in the same way. In Figure 3, we show the relationship between the social welfare in OP and in LF, as well as the ratio of the two quantities, and the hospital resources reallocated from city 2 to city 1.

The total welfare ratio of optimal policy to laissez-faire equilibrium is always larger than 1, which means total welfare is always improved when the decisions are made collectively by social planner. This improvement is approximately 25% to 27%, which can be considered as a very significant result. Moreover, when we go on with the discussion in the previous section, we can see that social welfare improves when part of the hospital resources in city 2 are moved to city 1, which further proves the necessity of resource re-allocations. In addition, from the figure we see that the welfare ratio peaks when the hospital resources allocated in city 1 are about 2,500 units, and then begins to decrease. This means that there exists an optimal allocation of the resources between the two cities, where the optimal policy can achieve the largest improvement of welfare compared with the results derived from laissez-faire equilibrium.

In this research, we only consider the migration behavior and omit the lockdown policy that many countries carry out during this pandemic. By including this into the consideration of public policy, it will further improve the social welfare.

4.4 Misallocation in a Pandemic

In this subsection, we go further to derive some additional results through numerical analysis to show that our model is consistent with the empirical findings shown in Table 1. The parameters of the model take the same values as in previous sections, with the exception that we now study different combinations of agents in different cities and extend the model to more than three cities. Moreover, in an n-city model when n is very large, we have to set an upper limit of migration rates ($\eta_{\max}$) to ensure that the sum of all the migration rates out of a city is not greater than 1. Then, the natural migration rates between each two cities become $\eta_{\max}/(n-1)$, where n is the total number of cities. The migration fee rates k are also adjusted correspondingly. Finally, we calculate the following indexes and compare them with the incentive facts shown in Section 1: normalized standard deviation of death rates in each city, total death rates, as well as deaths and cases per 10,000 people. The results are shown in Table 4.[4]

In addition to the benchmark model we use in this paper, it is also useful to study a model with no contagion, so as to show the differences coming from contagion externality. In Appendix C, we build a model with no contagion and derive the corresponding migration decisions made by agents and the social planner, respectively. In this model, migration rates of susceptible agents remain the natural level, since they can no longer be infected. On the other hand, infected agents still need to determine their optimal migration rates, in order to maximize their possibilities of being cured and minimize their death rates. Similarly, we can also derive a linear system of equations on the migration rates of infected agents in this model, which is

[4]In Appendix E, we also present the component of different types of agents in each city in pie graphs, in order to show the different results in laissez-faire equilibrium and optimal policy.

shown in Table A.1. Then, we can calculate the key variable—normalized standard deviation of death rates in each city—of this no-contagion model, and show them in the last column of Table 4, together with the corresponding results of the benchmark model.

We present five cases with different combinations of city types, from the case of a model with only three cities to that of thirty cities. From the observation of all the cases we can draw the following conclusions: The death rate, deaths and cases per 10,000 people, are always higher in laissez-faire equilibrium than in optimal policy; while the relationship is opposite regarding normalized standard deviation (SD) of death rate. These observations are consistent with what we find from the data: The normalized SD of the death rates for countries with a lower number of cases and deaths such as China, South Korea and Japan (we consider these countries in a state close to the optimal level) is much more higher than in countries with poorer performance in dealing with the pandemic like the U.S., Brazil and India (we consider these countries in a state close to a laissez-faire equilibrium). Moreover, we can further illustrate the misallocation problem by comparing the normalized standard deviation of death rate of the benchmark model and the no-contagion model (see the last two column in Table 4). When there is no contagion, this key variable decreases significantly in optimal policy, while in laissez-faire equilibrium, it becomes very close to the results in the former situation. The differences between the two situations in the no-contagion model just come from the crowding-out effect of hospital resources, and they are rather small compared with those coming from contagion externality in the benchmark model. The comparison of the two models further shows that misallocation can be somewhat desirable when some kind of serious externality arises, while in most of the cases, resource equalization is the optimal case.

Finally, we should point out that rearranging the migrations is not the only way to deal with a pandemic for the government. Another effective method to deal with the pandemic is the lockdown policy. As this policy has been widely discussed in the literature, we have only studied in this paper the net effect of migration policy, which explains part of the differences.

5 Conclusions

In this research, we develop an endogenous migration model during pandemics with hospital resource constraints, integrated with a traditional SIR model. The uneven distribution of medical resources across cities and regions induces large-scale migrations which can exacerbate the spread of the virus. On the other hand, migrations can help to equalize the amount of medical resources per capita throughout the different areas, mitigating the resource misallocation problem. Therefore, migration can alleviate resource misallocation but also exacerbate the pandemic, leading to the existence of some kind of trade-off in terms of migration control from the policy perspective

In our model, several explicit solutions on migration decisions are provided, and we further use these results to study the relationship between allocation of hospital resources and migration decisions. By comparing the results of the laissez-faire equilibrium with the optimal policy, we find that migration decisions made by agents independently are somewhat different from the optimal policy, especially for those infected agents living in the epidemic focus of the pandemic. In addition, the simulated results are consistent with what we find from the data, which further support the effectiveness of our model. The framework we develop can be used to understand the behavior of people when facing an unknown epidemic disease like COVID-19, and provide a tool for governments to efficiently allocate hospital resources and different types of agents during these uncertain times.

References

Acemoglu, D., Chernozhukov, V., Werning, I., and Whinston, M. D. (2020). A Multi-Risk SIR Model with Optimally Targeted Lockdown. Unpublished.

Alvarez, F., Argente, D., and Lippi, F. (2021). A Simple Planning Problem for COVID-19 Lock-down, Testing, and Tracing. *American Economic Review: Insights*, 3(3):367–382.

Bisin, A. and Moro, A. (2020). Learning Epidemiology by Doing: The Empirical Implications of a Spatial-SIR Model with Behavioral Responses. Working paper 27590, National Bureau of Economic Research.

Bobashev, G., Cropper, M. L., Epstein, J. M., Goedecke, D. M., Hutton, S., and Over, M. (2011). Policy Response to Pandemic Influenza: The Value of Collection Action. Working paper 17195, National Bureau of Economic Research.

Chan, T. Y., Hamilton, B. H., and Papageorge, N. W. (2016). Health, Risky Behaviour and the Value of Medical Innovation for Infectious Disease. *Review of Economic Studies*, 83(4):1465–1510.

Chinazzi, M., Davis, J. T., Ajelli, M., Gioannini, C., Litvinova, M., Merler, S., y Piontti, A. P., Mu, K., Rossi, L., Sun, K., Viboud, C., Xiong, X., Yu, H., Halloran, M. E., Jr., I. M. L., and Vespignani, A. (2020). The Effect of Travel Restrictions on the Spread of the 2019 Novel Coronavirus (COVID-19) Outbreak. *Science*, 368(6489):395–400.

Chowell, G., Fenimore, P. W., Castillo-Garsow, M. A., and Castillo-Chavez, C. (2003). SARS Outbreaks in Ontario, Hong Kong and Singapore: The Role of Diagnosis and Isolation as a Control Mechanism. *Journal of Theoretical Biology*, 224(1):1–8.

Dower, P. C. and Markevich, A. (2018). Labor Misallocation and Mass Mobilization: Russian Agriculture during the Great War. *Review of Economics and Statistics*, 100(2):245–259.

Eichenbaum, M. S., Rebelo, S., and Trabandt, M. (2021). The Macroeconomics of Epidemics. *Review of Financial Studies*, 34:5149–5187.

Fajgelbaum, P., Khandelwal, A., Kim, W., Mantovani, C., and Schaal, E. (2020). Optimal Lockdown in a Commuting Network. Working paper 27441, National Bureau of Economic Research.

Fang, H., Wang, L., and Yang, Y. (2020). Human Mobility Restrictions and the Spread of the Novel Coronavirus (2019-nCoV) in China. *Journal of Public Economics*, 191:104272.

Farboodi, M., Jarosch, G., and Shimer, R. (2020). Internal and External Effects of Social Distancing in a Pandemic. Working paper 27059, National Bureau of Economic Research.

Fernàndez-Villaverde, J. and Jones, C. I. (2020). Estimating and Simulating a SIRD Model of COVID-19 for Many Countries, States, and Cities. Unpublished.

Grossman, M. (1972). On the Concept of Health Capital and the Demand for Health. *Journal of Political Economy*, 80(2):223–255.

Guerrieri, V., Lorenzoni, G., Straub, L., and Werning, I. (2020). Macroeconomic Implications of COVID-19: Can Negative Supply Shocks Cause Demand Shortages? Working paper 26918, National Bureau of Economic Research.

Hall, R. E., Jones, C. I., and Klenow, P. J. (2020). Trading Off Consumption and COVID-19 Deaths. Unpublished.

Hsieh, C.-T., Hurst, E., Jones, C. I., and Klenow, P. J. (2019). The Allocation of Talent and U.S. Economic Growth. *Econometrica*, 87(5):1439–1474.

Hsieh, C.-T. and Klenow, P. J. (2009). Misallocation and Manufacturing TFP in China and India. *Quarterly Journal of Economics*, 124(4):1403–1448.

Jones, C. J., Philippon, T., and Venkateswaran, V. (2021). Optimal Mitigation Policies in a Pandemic: Social Distancing and Working from Home. *Review of Financial Studies*, 34:5188–5223.

Kermack, W. O., McKendrick, A. G., and Walker, G. T. (1927). A Contribution to the Mathematical Theory of Epidemics. *Proceedings of the Royal Society of London. Series A, Containing Papers of a Mathematical and Physical Character*, 115(772):700–721.

Stehlé, J., Voirin, N., Barrat, A., Cattuto, C., Colizza, V., Isella, L., Régis, C., Pinton, J.-F., Khanafer, N., Van Den Broeck, W., and Vanhems, P. (2011). Simulation of an SEIR Infectious Disease Model on the Dynamic Contact Network of Conference Attendees. *BMC Medicine*, 9(1):87.

Tombe, T. and Zhu, X. (2019). Trade, Migration, and Productivity: A Quantitative Analysis of China. *American Economic Review*, 109(5).

Yang, Z., Zeng, Z., Wang, K., Wong, S.-S., Liang, W., Zanin, M., Liu, P., Cao, X., Gao, Z., Mai, Z., Liang, J., Liu, X., Li, S., Li, Y., Ye, F., Guan, W., Yang, Y., Li, F., Luo, S., Xie, Y., Liu, B., Wang, Z., Zhang, S., Wang, Y., Zhong, N., and He, J. (2020). Modified SEIR and AI Prediction of the Epidemics Trend of COVID-19 in China under Public Health Interventions. *Journal of Thoracic Disease*, 12(3):165–174.

6 Figures and Tables

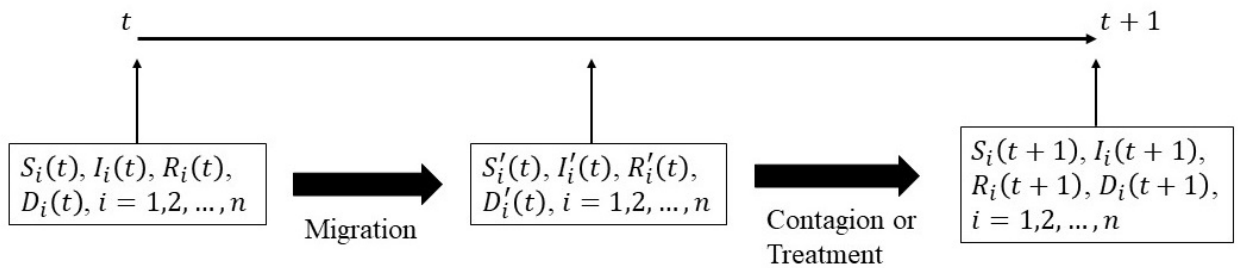

Figure 1: Timeline of the Model

Notes. This figure shows the timeline of our model. From period t to $t+1$, agents in different cities first make the decisions of migration, and then are infected or treated in their new cities, depending on the states they are in. The aggregate number of different types of agents change according to these decisions.

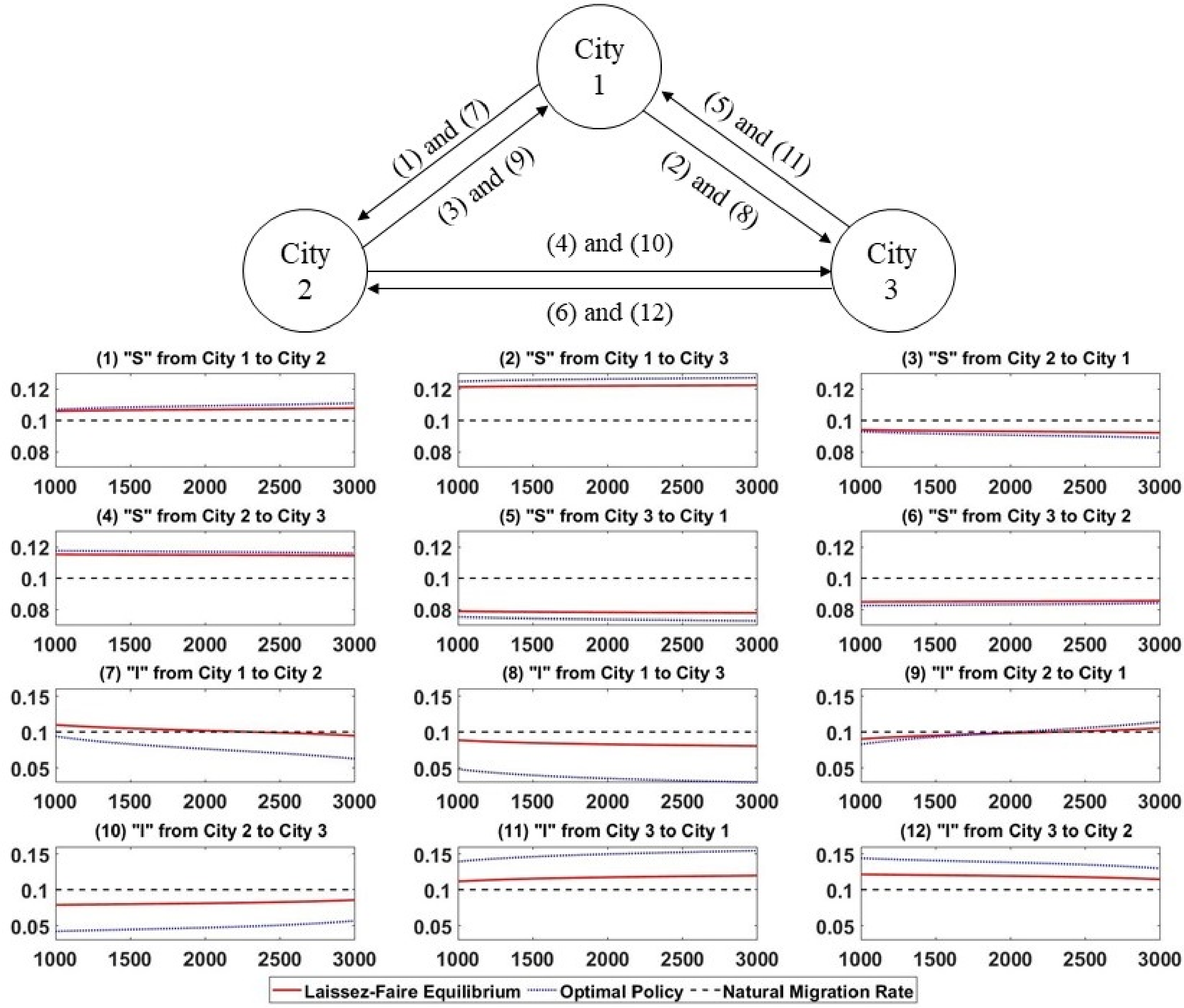

Figure 2: Relationship between Migration Rates and the Hospital Resources Allocated in city 1.

Notes. The triangle above shows the corresponding relationship between the migration rates and the panels shown below. The panels (1)-(12) show the relationship between migration rates of all types of agents in the three cities and the hospital resources allocated in city 1, with the x-axis represents the hospital resources allocated in city 1, and the y-axis represents the migration rates (All the panels from (1) to (6) and from (7) to (12) are set in the same range, respectively). Moreover, the solid lines represent the decisions made by agents independently in the laissez-faire equilibrium, the dotted lines represent the collective actions taken by the central government in the optimal policy, and the dash lines represent the natural migration rate for reference. We should note that when the hospital resources in city 1 increase, resources in city 2 decrease accordingly. Numbers of different types of agents in these three cities are set as the following: $S_1 = 0.457N$, $I_1 = 0.3N$, $R_1 = 0.24N$, $D_1 = 0.003N$, $S_2 = 0.638N$, $I_2 = 0.2N$, $R_2 = 0.16N$, $D_2 = 0.002N$, $S_3 = 0.99N$, $I_3 = 0.008N$, $R_3 = 0.002N$, $D_3 = 0$.

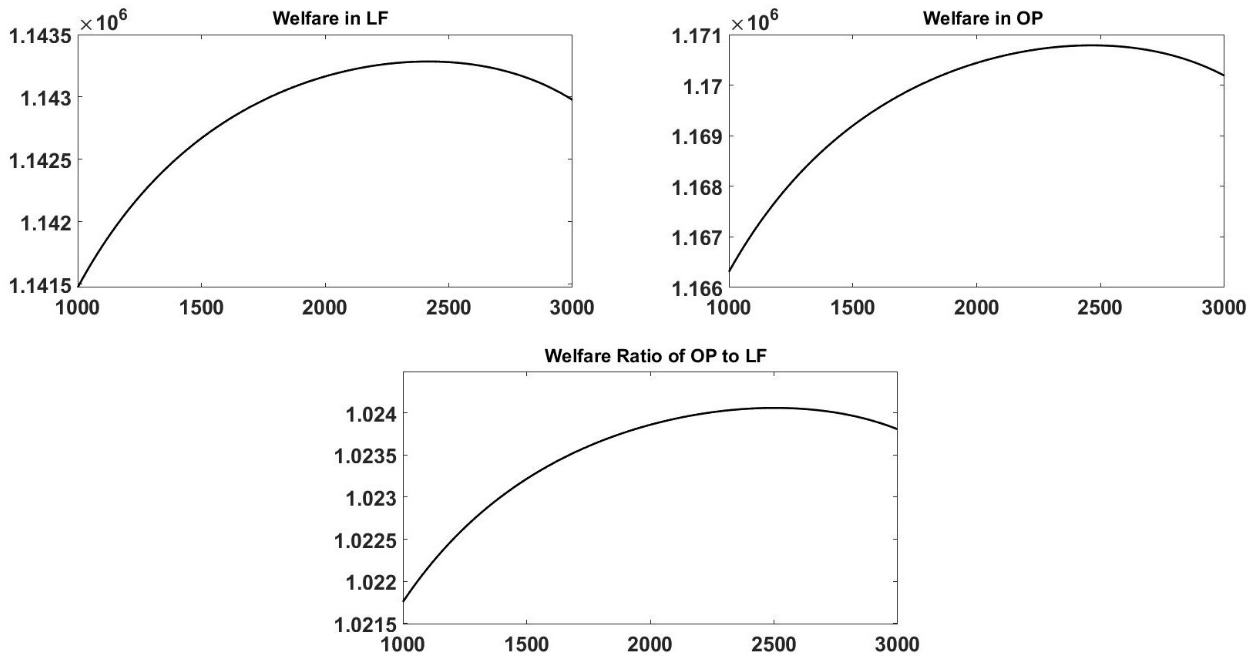

Figure 3: Relationship between Total Welfare and the Hospital Resources Allocated in city 1, Two-Week Time Span

Notes. The first two panels show the relationship between total welfare and the hospital resources allocated in city 1, in the laissez-faire equilibrium (LF) and in the optimal policy (OP), respectively. The third panel shows the relationship between the welfare ratio of OP to LF and the resources allocation. The x-axis represents the hospital resources in city 1. We should note that when the resources in city 1 increase, resources in city 2 decrease accordingly. Parameters used in calculating this result are all the same as those used in Figure 2.

Table 1: Heterogeneous COVID-19 Death Rates

Countries (Provinces)	Date	Cases	Deaths	$\frac{\text{Deaths}}{\text{Cases}}$	Deaths per 100k People	Normalized SD of Death Rate	Hospital Beds per 1k People
Cross-Country Comparison							
United States	Aug. 26th	5,343,498	145,803	2.73%	45	0.69	2.9
India	Aug. 27th	3,234,474	59,449	1.84%	4.4	0.75	0.7
Brazil	Aug. 26th	3,717,156	117,665	3.17%	56	0.49	2.2
Germany	Aug. 21th	230,048	9,260	4.03%	11	0.23	8.3
South Korea	Aug. 26th	16,620	310	1.87%	0.60	1.11	11.5
Japan	Aug. 26th	63,973	1,229	1.92%	0.97	1.01	13.4
Mainland China	Aug. 2th	83,882	4,634	5.52%	0.33	1.23	4.2
Comparison within Mainland China							
Hubei	Aug. 2th	68,135	4,512	6.62%	7.6	-	6.7
(Wuhan of Hubei)	Aug. 2th	50,340	3,869	7.69%	35	-	9.2
Henan	Aug. 2th	1,276	22	1.72%	0.022	-	6.3
Heilongjiang	Aug. 2th	947	13	1.37%	0.034	-	6.6
Beijing	Aug. 2th	929	9	0.97%	0.042	-	9.1
Guangdong	Aug. 2th	1,672	8	0.48%	0.007	-	4.6
Shandong	Aug. 2th	799	7	0.88%	0.007	-	6.1
Shanghai	Aug. 2th	741	7	0.94%	0.029	-	9.6

Data Source: Official statistics of China and other countries, Wikipedia, and Johns Hopkins University Center for Systems Science and Engineering. Hospital beds per thousand people of different countries are the data in 2016. The standard deviation (SD) of death rate is calculated from the state-level statistics, and the normalized SD is calculated by dividing the SD by the corresponding state-level mean statistics. As for the comparison within mainland China, we only show the seven provinces with the largest mortality, as well as Wuhan which is the provincial capital of Hubei Province and the epidemic focus of the disease.

Table 2: Elements in the Transition Matrix

Health states in current period	Health states in the last period			
	S_i	I_i	R_i	D_i
S_i	$\left(1 - \sum_{k \neq i} \tilde{\eta}_{S,ik}\right)(1 - p_{i,t})$	0	0	0
I_i	$\left(1 - \sum_{k \neq i} \tilde{\eta}_{S,ik}\right) p_{i,t}$	$\left(1 - \sum_{k \neq i} \tilde{\eta}_{I,ik}\right)(1 - q_{i,t} - r_{i,t})$	0	0
R_i	0	$\left(1 - \sum_{k \neq i} \tilde{\eta}_{I,ik}\right) q_{i,t}$	$1 - \sum_{k \neq i} \bar{\eta}_{ik}$	0
D_i	0	$\left(1 - \sum_{k \neq i} \tilde{\eta}_{I,ik}\right) r_{i,t}$	0	1
S_j	$\tilde{\eta}_{S,ij}(1 - p_{j,t})$	0	0	0
I_j	$\tilde{\eta}_{S,ij} p_{j,t}$	$\tilde{\eta}_{I,ij}(1 - q_{j,t} - r_{j,t})$	0	0
R_j	0	$\tilde{\eta}_{I,ij} q_{j,t}$	$\bar{\eta}_{ij}$	0
D_j	0	$\tilde{\eta}_{I,ij} r_{j,t}$	0	0

Note. The size of the transition matrix is $4n \times 4n$, with four types of agents in each of the n cities. For the convenience of presentation, we show the matrix in the form of a table (for any $i, j = 1, 2, ..., n$ and $j \neq i$).

Table 3: Elements in the Matrix $\boldsymbol{A}$ and Vector $\boldsymbol{B}$ in Laissez-Faire Equilibrium and in Optimal Policy

Elements in Matrix $\boldsymbol{A}$

Column	Row $(U, ij), U = S, I$			
	Laissez-Faire Equilibrium, $\boldsymbol{A}_L$		Optimal Policy, $\boldsymbol{A}_O$	
	(S, ij)	(I, ij)	(S, ij)	(I, ij)
(S, ij)	1	0	1	$\frac{C_S S_i}{k_{ij}} \left(\frac{1}{N_i - D_i} + \frac{1}{N_j - D_j} \right)$
(S, ji)	0	0	0	$-\frac{C_S S_j}{k_{ij}} \left(\frac{1}{N_i - D_i} + \frac{1}{N_j - D_j} \right)$
(S, ik)	0	0	0	$\frac{1}{k_{ij}} C_S \frac{S_i}{N_i - D_i}$
(S, ki)	0	0	0	0
(S, jk)	0	0	0	$-\frac{1}{k_{ij}} C_S \frac{S_j}{N_j - D_j}$
(S, kj)	0	0	0	0
(I, ij)	$\frac{C_S I_i}{k_{ij}} \left(\frac{1}{N_i - D_i} + \frac{1}{N_j - D_j} \right)$	$\frac{C_I I_i}{k_{ij}} \left(\frac{1}{H_i} + \frac{1}{H_j} \right) + 1$	$\frac{C_S I_i}{k_{ij}} \left(\frac{1}{N_i - D_i} + \frac{1}{N_j - D_j} \right)$	$\frac{C_I I_i}{k_{ij}} \left(\frac{1}{H_i} + \frac{1}{H_j} \right) + 1$
(I, ji)	$-\frac{C_S I_j}{k_{ij}} \left(\frac{1}{N_i - D_i} + \frac{1}{N_j - D_j} \right)$	$-\frac{C_I I_j}{k_{ij}} \left(\frac{1}{H_i} + \frac{1}{H_j} \right)$	$-\frac{C_S I_j}{k_{ij}} \left(\frac{1}{N_i - D_i} + \frac{1}{N_j - D_j} \right)$	$-\frac{2C_I I_j}{k_{ij}} \left(\frac{1}{H_i} + \frac{1}{H_j} \right)$
(I, ik)	$\frac{1}{k_{ij}} C_S \frac{I_i}{N_i - D_i}$	$\frac{1}{k_{ij}} C_I \frac{I_i}{H_i}$	$\frac{1}{k_{ij}} C_S \frac{I_i}{N_i - D_i}$	$\frac{2}{k_{ij}} C_I \frac{I_i}{H_i}$
(I, ki)	$-\frac{1}{k_{ij}} C_S \frac{I_k}{N_i - D_i}$	$-\frac{1}{k_{ij}} C_I \frac{I_k}{H_i}$	$-\frac{1}{k_{ij}} C_S \frac{I_k}{N_i - D_i}$	$-\frac{2}{k_{ij}} C_I \frac{I_k}{H_i}$
(I, jk)	$-\frac{1}{k_{ij}} C_S \frac{I_j}{N_j - D_j}$	$-\frac{1}{k_{ij}} C_I \frac{I_j}{H_j}$	$-\frac{1}{k_{ij}} C_S \frac{I_j}{N_j - D_j}$	$-\frac{2}{k_{ij}} C_I \frac{I_j}{H_j}$
(I, kj)	$\frac{1}{k_{ij}} C_S \frac{I_k}{N_j - D_j}$	$\frac{1}{k_{ij}} C_I \frac{I_k}{H_j}$	$\frac{1}{k_{ij}} C_S \frac{I_k}{N_j - D_j}$	$\frac{1}{k_{ij}} C_I \frac{I_k}{H_j}$
(S, kl)	0	0	0	0
(I, kl)	0	0	0	0

Elements in Vector $\boldsymbol{B}$

	Laissez-Faire Equilibrium, $\boldsymbol{B}_L$	Optimal Policy, $\boldsymbol{B}_O$
$B_{(S,ij)}$	$\frac{1}{k_{ij}} C_S \left(\frac{I_i}{N_i - D_i} - \frac{I_j}{N_j - D_j} \right) + \bar{\eta}_{ij}$	$\frac{1}{k_{ij}} C_S \left(\frac{I_i}{N_i - D_i} - \frac{I_j}{N_j - D_j} \right) + \bar{\eta}_{ij}$
$B_{(I,ij)}$	$\frac{1}{k_{ij}} C_I \left(\frac{I_i}{H_i} - \frac{I_j}{H_j} \right) + \bar{\eta}_{ij}$	$\frac{1}{k_{ij}} C_S \left(\frac{S_i}{N_i - D_i} - \frac{S_j}{N_j - D_j} \right) + \frac{2}{k_{ij}} C_I \left(\frac{I_i}{H_i} - \frac{I_j}{H_j} \right) + \bar{\eta}_{ij}$

Note. The solution of migration rates can be derived from a system of linear equations $\boldsymbol{A}\boldsymbol{\eta} = \boldsymbol{B}$. Here, the size of matrix $\boldsymbol{A}$ is $2n(n-1) \times 2n(n-1)$, and the size of vector $\boldsymbol{B}$ is $2n(n-1) \times 1$. There are in total $2n(n-1)$ different migration rates to be solved, with two types of agents (susceptible and infected) in each of the n cities, and each agent selects the migration rates from the city they live in to the other $(n-1)$ cities. For the convenience of presentation, we show the matrix in the form of a table (for any $i, j, k, l = 1, 2, ..., n$, and these four numbers are different from each other). C_S and C_I are shown in (9) and (10), respectively.

Table 4: Simulated Results in Different Cases, Two-Week Time Span

Cases	Initial Number of Different Types of Agents and Hospital Resources	States	$\frac{\text{Deaths}}{\text{Cases}}$	Deaths per 10k People	Cases per 10k People	Normalized Standard Deviation of Death Rate	
						With Contagion	No Contagion
I	1 epidemic focus +	Initial	0.53%	10	1,048	1.3693	1.3693
($n = 5$,	1 large city +	LF	0.71%	41.17	4,735	0.2202	0.1517
$\eta_{max} = 0.8$)	3 small cities	OP	2.21%	36.47	513	1.7829	0.1377
II	1 epidemic focus +	Initial	0.54%	13	1332	0.8607	0.8607
($n = 10$,	5 large city +	LF	0.68%	51.22	6,192	0.3383	0.3237
$\eta_{max} = 0.8$)	4 small cities	OP	0.60%	38.43	4,575	0.9202	0.3196
III	1 epidemic focus +	Initial	0.52%	7	706	1.5672	1.5672
($n = 20$,	5 large cities +	LF	0.66%	30.22	3,971	0.1380	0.1353
$\eta_{max} = 0.8$)	14 small cities	OP	0.48%	20.67	3,104	0.5424	0.1217
IV	1 epidemic focus +	Initial	0.53%	7	817	1.3367	1.3367
($n = 30$,	10 large cities +	LF	0.68%	36.09	4,546	0.2103	0.2213
$\eta_{max} = 0.8$)	19 small cities	OP	0.49%	26.22	4,041	0.2283	0.1820
V	1 epidemic focus +	Initial	0.51%	4.60	384	1.9021	1.9021
($n = 50$,	10 large cities +	LF	0.59%	20.95	3,049	0.0463	0.0493
$\eta_{max} = 0.8$)	39 small cities	OP	0.45%	17.52	2,901	0.1731	0.1145

Note. This table shows various simulated results from numerical analysis, including indexes in the initial state, the laissez-faire equilibrium (LF) and the optimal policy (OP). In addition to the benchmark model, we also provide the normalized SD of death rate when there is no contagion. For simplicity, we only consider three types of cities with different combinations of agent types and hospital resources here: epidemic focus (with largest number of infected agents but median hospital resources, $S_1 = 0.457N$, $I_1 = 0.3N$, $R_1 = 0.24N$, $D_1 = 0.003N$, $H_1 = 0.1N$), large city (with median number of infected agents but most abundant hospital resources, $S_2 = 0.638N$, $I_2 = 0.2N$, $R_2 = 0.16N$, $D_2 = 0.002N$, $H_2 = 0.3N$) and small city (with little number of infected agents and little hospital resources, $S_3 = 0.99N$, $I_3 = 0.008N$, $R_3 = 0.002N$, $D_3 = 0$, $H_3 = 0.01N$).

Appendix A Derivation of Migration Rates in Laissez-Faire Equilibrium

Agents of different types maximize their utilities separately. Formally, for susceptible ones in city i, the optimal migration rate is

$$\tilde{\eta}_{S,ij} = \bar{\eta}_{ij} + \frac{\phi}{2k_{ij}}(p_{i,t} - p_{j,t})(1 - u_I). \tag{A.1}$$

Similarly, we can derive the migration rates determined by the infected agents in city i as

$$\tilde{\eta}_{I,ij} = \bar{\eta}_{ij} + \frac{\phi}{2k_{ij}}[(q_{j,t} - q_{i,t})(1 - u_I) + (r_{i,t} - r_{j,t})(u_I - u_D)]. \tag{A.2}$$

A rational expectation equilibrium is that, the optimal decisions of different agents equal to the aggregate decisions of the corresponding types of agents, i.e., $\tilde{\eta}_{S,ij} = \eta_{S,ij}$, $\tilde{\eta}_{I,ij} = \eta_{I,ij}$, $i, j = 1, 2, ..., n$. Then, we can pin down the migration rates through (A.1) and (A.2), which is shown in Table 3.

Appendix B Derivation of Migration Rates in Social Optimal Policy

First, we derive the first-order derivatives of the utility function. The derivatives between different infected rates p and different migration rates η^* are shown as follows. For any combinations that satisfy $i, j = 1, 2, ..., n$, $i \neq j$, we have

$$\frac{\partial p_{i,t}}{\partial \eta^*_{I,ij}} = -\beta \frac{I_i}{N_i - D_i} \tag{A.3}$$

and

$$\frac{\partial p_{i,t}}{\partial \eta^*_{I,ji}} = \beta \frac{I_j}{N_i - D_i}. \tag{A.4}$$

For any combinations that satisfy $i, j, k = 1, 2, ..., n$ and i, j, k are different from each other, we have

$$\frac{\partial p_{i,t}}{\partial \eta^*_{I,jk}} = 0. \tag{A.5}$$

On the other hand, the derivatives between different recovering rates q and different migration rates η^* are shown as follows. For any combinations that satisfy $i, j = 1, 2, ..., n$, $i \neq j$, we have

$$\frac{\partial q_{i,t}}{\partial \eta^*_{I,ij}} = \kappa_1 \frac{I_i}{H_i} \tag{A.6}$$

and

$$\frac{\partial q_{i,t}}{\partial \eta^*_{I,ji}} = -\kappa_1 \frac{I_j}{H_i}. \tag{A.7}$$

For any combinations that satisfy $i, j, k = 1, 2, ..., n$ and i, j, k are different from each other, we have

$$\frac{\partial q_{i,t}}{\partial \eta^*_{I,jk}} = 0. \tag{A.8}$$

Finally, the derivatives between different death rates r and different migration rates η^* are shown as follows. For any combinations that satisfy $i, j = 1, 2, ..., n$, $i \neq j$, we have

$$\frac{\partial r_{i,t}}{\partial \eta^*_{I,ij}} = -\kappa_2 \frac{I_i}{H_i} \tag{A.9}$$

and

$$\frac{\partial r_{i,t}}{\partial \eta^*_{I,ji}} = \kappa_2 \frac{I_j}{H_i}. \tag{A.10}$$

For any combinations that satisfy $i, j, k = 1, 2, ..., n$ and i, j, k are different from each other, we have

$$\frac{\partial r_{i,t}}{\partial \eta^*_{I,jk}} = 0. \tag{A.11}$$

As a result, the FOCs with respect to all the migration rates are shown as follows. For any combinations that satisfy $i, j = 1, 2, ..., n$, $i \neq j$, we have

$$\frac{\partial U}{\partial \eta^*_{S,ij}} = S_i \left[-2k_{ij}(\eta^*_{S,ij} - \bar{\eta}_{ij}) + \phi(1 - u_I)(p_{i,t} - p_{j,t}) \right] = 0 \tag{A.12}$$

and

$$\begin{aligned}
\frac{\partial U}{\partial \eta^*_{I,ij}} =& I_i \phi \beta \left[\frac{\left(1 - \sum_{k \neq i} \eta^*_{S,ik}\right) S_i + \eta^*_{S,ji} S_j}{N_i - D_i} - \frac{\eta^*_{S,ij} S_i + \left(1 - \sum_{k \neq j} \eta^*_{S,jk}\right) S_j}{N_j - D_j} \right] \\
& - 2k_{ij} I_i (\eta^*_{I,ij} - \bar{\eta}_{ij}) + \phi \left[(1 - u_I)\kappa_1 + (u_I - u_D)\kappa_2 \right] I_i \left\{ \left[\frac{2\left(1 - \sum_{k \neq i} \eta^*_{I,ik}\right) I_i + \sum_{k \neq i} \eta^*_{I,ki} I_k}{H_i} \right. \right. \\
& \left. - \frac{2 \sum_{k \neq j} \eta^*_{I,kj} I_k + \left(1 - \sum_{k \neq j} \eta^*_{I,jk}\right) I_j}{H_j} \right] + I_j \left(\frac{\eta^*_{I,ji}}{H_i} - \frac{1 - \sum_{k \neq j} \eta^*_{I,jk}}{H_j} \right) \\
& \left. + \sum_{k \neq i,j} \left[I_k \left(\frac{\eta^*_{I,ki}}{H_i} + \frac{\eta^*_{I,kj}}{H_j} \right) \right] \right\} = 0.
\end{aligned} \tag{A.13}$$

Based on the FOCs derived above, we then have the system of linear equations that determines the social optimal migration rates, which is shown in Table 3.

Appendix C Migration Decisions with No Contagion

If the disease becomes not contagious from a certain period on, that is, susceptible agents no longer need to worry about being infected by the infected agents. As a result, their migration decisions will return to the natural level from then on. Given the same initial number of different types of agents as we use in the benchmark model, we now only need to derive the migration decisions of infected ones in both situations of laissez-faire equilibrium and optimal policy. As for the former situation, the optimal decisions of infected agents can be derived from (A.2) and let the individual decision equals the aggregate decision. On the other hand, as for the latter situation, we should change the derivation in the benchmark model a little bit to get the result.

With no contagion, the expected utility (11) is now written as

$$
\begin{aligned}
&E[U(c_{1,t},...,c_{j,t},...;h_{1,t},...,h_{j,t},...)|\mathscr{F}_{t-1}] \\
=&\sum_{i=1}^{n} I_i \left\{ w - f(\eta^*_{I,ij}; j\neq i) + \phi \left[\left(1-\sum_{j\neq i}\eta^*_{I,ij}\right)(1-q_{i,t}-r_{i,t})u_I + \left(1-\sum_{j\neq i}\eta^*_{I,ij}\right) q_{i,t} \right.\right. \\
&\left.\left. + \left(1-\sum_{j\neq i}\eta^*_{I,ij}\right) r_{i,t}u_D + \sum_{j\neq i}(\eta^*_{I,ij}(1-q_{j,t}-r_{j,t})u_I + \eta^*_{I,ij}q_{j,t} + \eta^*_{I,ij}r_{j,t}u_D)\right]\right\} \\
&+\sum_{i=1}^{n}\left[S_i(w+\phi)+R_i(w+\phi)+D_i(w+\phi u_D)\right]. \qquad \text{(A.14)}
\end{aligned}
$$

Then, the FOCs with respect to all the migration rates of infected agents can be derived from (A.14). For any combinations that satisfy $i, j = 1, 2, ..., n.i \neq j$, we have

$$
\begin{aligned}
\frac{\partial U}{\partial \eta^*_{I,ij}} =& -2k_{ij}I_i(\eta^*_{I,ij}-\bar{\eta}_{ij}) + \phi\left[(1-u_I)\kappa_1+(u_I-u_D)\kappa_2\right] I_i \left\{ \left[\frac{2\left(1-\sum_{k\neq i}\eta^*_{I,ik}\right)I_i + \sum_{k\neq i}\eta^*_{I,ki}I_k}{H_i} \right.\right. \\
&\left. - \frac{2\sum_{k\neq j}\eta^*_{I,kj}I_k + \left(1-\sum_{k\neq j}\eta^*_{I,jk}\right)I_j}{H_j} \right] + I_j\left(\frac{\eta^*_{I,ji}}{H_i} - \frac{1-\sum_{k\neq j}\eta^*_{I,jk}}{H_j}\right) \\
&\left. + \sum_{k\neq i,j}\left[I_k\left(\frac{\eta^*_{I,ki}}{H_i}+\frac{\eta^*_{I,kj}}{H_j}\right)\right]\right\} = 0. \qquad \text{(A.15)}
\end{aligned}
$$

Based on the FOCs derived above, we then have the system of linear equations that determines the optimal migration rates with no contagion. The results of the benchmark model shown in Table 3 is now simplified, which is shown in Table A.1.

Table A.1: Elements in the Matrix $\boldsymbol{A}$ and Vector $\boldsymbol{B}$ in Laissez-Faire Equilibrium and in Optimal Policy (No Contagion)

Elements in Matrix $\boldsymbol{A}$		
	Row (I, ij)	
Column	Laissez-Faire Equilibrium, $\boldsymbol{A}_L$	Optimal Policy, $\boldsymbol{A}_O$
	(I, ij)	(I, ij)
(I, ij)	$\frac{C_I I_i}{k_{ij}}\left(\frac{1}{H_i}+\frac{1}{H_j}\right)+1$	$\frac{C_I I_i}{k_{ij}}\left(\frac{1}{H_i}+\frac{1}{H_j}\right)+1$
(I, ji)	$-\frac{C_I I_j}{k_{ij}}\left(\frac{1}{H_i}+\frac{1}{H_j}\right)$	$-\frac{2C_I I_j}{k_{ij}}\left(\frac{1}{H_i}+\frac{1}{H_j}\right)$
(I, ik)	$\frac{1}{k_{ij}}C_I\frac{I_i}{H_i}$	$\frac{2}{k_{ij}}C_I\frac{I_i}{H_i}$
(I, ki)	$-\frac{1}{k_{ij}}C_I\frac{I_k}{H_i}$	$-\frac{2}{k_{ij}}C_I\frac{I_k}{H_i}$
(I, jk)	$-\frac{1}{k_{ij}}C_I\frac{I_j}{H_j}$	$-\frac{2}{k_{ij}}C_I\frac{I_j}{H_j}$
(I, kj)	$\frac{1}{k_{ij}}C_I\frac{I_k}{H_j}$	$\frac{1}{k_{ij}}C_I\frac{I_k}{H_j}$
(I, kl)	0	0
Elements in Vector $\boldsymbol{B}$		
	Laissez-Faire Equilibrium, $\boldsymbol{B}_L$	Optimal Policy, $\boldsymbol{B}_O$
$B_{(I,ij)}$	$\frac{1}{k_{ij}}C_I\left(\frac{I_i}{H_i}-\frac{I_j}{H_j}\right)+\bar{\eta}_{ij}$	$\frac{2}{k_{ij}}C_I\left(\frac{I_i}{H_i}-\frac{I_j}{H_j}\right)+\bar{\eta}_{ij}$

Note. The solution of migration rates can be derived from a system of linear equations $\boldsymbol{A\eta} = \boldsymbol{B}$. Here, the size of matrix $\boldsymbol{A}$ is $n(n-1) \times n(n-1)$, and the size of vector $\boldsymbol{B}$ is $n(n-1) \times 1$. There are in total $n(n-1)$ different migration rates to be solved, with infected agents in each of the n cities, and each agent selects the migration rates from the city they live in to the other $(n-1)$ cities. For the convenience of presentation, we show the matrix in the form of a table (for any $i, j, k, l = 1, 2, ..., n$, and these four numbers are different from each other). C_I is shown in (10).

In Table 4, we show the corresponding results derived in this section, in addition to the results derived from the benchmark model.

Appendix D Influence of Hospital Resources Allocation to Migration Decisions

If we simplify the n-city model presented in the main text into a two-city one, the relationship can be derived analytically in laissez-faire equilibrium. As a result, we have the following proposition.

Proposition D.1. *In a model with only two cities, in the laissez-faire equilibrium, in response to an increase in hospital resources in city 1, susceptible agents in this city will be more inclined to move to another city while those infected will be more inclined to stay in it.*

Proof. Rewrite the determine equations of migration rates (8) into the form of

$$\boldsymbol{A}\boldsymbol{\eta} - \boldsymbol{B} = \boldsymbol{F}(\boldsymbol{\eta}, H_1, H_2, ..., H_n) = 0. \tag{A.16}$$

Then, according to the general implicit function theorem, we have (for any $i, k, l = 1, 2, ..., n$, $k \neq l$, $U = S, I$)

$$\frac{\partial \eta_{U,kl}}{\partial H_i} = -\frac{\begin{vmatrix} \frac{\partial F_{S,12}}{\partial \eta_{S,12}} & \cdots & \frac{\partial F_{(S,12)}}{\partial H_i} & \cdots & \frac{\partial F_{S,12}}{\partial \eta_{I,(n-1)n}} \\ \frac{\partial F_{S,13}}{\partial \eta_{S,12}} & \cdots & \frac{\partial F_{(S,13)}}{\partial H_i} & \cdots & \frac{\partial F_{S,13}}{\partial \eta_{I,(n-1)n}} \\ \cdots & \cdots & \cdots & \cdots & \cdots \\ \frac{\partial F_{S,(n-1)n}}{\partial \eta_{S,12}} & \cdots & \frac{\partial F_{(I,(n-1)n)}}{\partial H_i} & \cdots & \frac{\partial F_{I,(n-1)n}}{\partial \eta_{I,(n-1)n}} \end{vmatrix}}{|\boldsymbol{A}|}, \tag{A.17}$$

Here, elements in the numerator is the same as those in the denominator, except that the column corresponding to $\eta_{U,kl}$, is replaced by derivatives with respect to the hospital resources in city i, which is what we are aiming to study in this appendix.

In laissez-faire equilibrium, determinate $|\boldsymbol{A}|$ is in a form like

$$|\boldsymbol{A}| = \begin{vmatrix} \boldsymbol{I}_{n(n-1)\times n(n-1)} & \boldsymbol{A}_{(S,ij),(I,kl)} \\ \boldsymbol{0}_{n(n-1)\times n(n-1)} & \boldsymbol{A}_{(I,ij),(I,kl)} \end{vmatrix}, \tag{A.18}$$

where, $\boldsymbol{I}_{n(n-1)\times n(n-1)}$ is a unit matrix.

First, we derive the derivatives with respect to H_i. For any terms that corresponding to (S, kl), we all have

$$\frac{\partial F_{(S,kl)}}{\partial H_i} = 0. \tag{A.19}$$

Meanwhile, for any terms that corresponding to (I, kl), we have to divide into two cases. For the term $F_{(I,ij)}$, we have

$$\frac{\partial F_{(I,ij)}}{\partial H_i} = -\frac{C_I}{k_{ij} H_i^2} \left[I_i \eta_{I,ij} - I_j \eta_{I,ji} + \sum_{k \neq i,j} (I_i \eta_{I,ik} - I_k \eta_{I,ki}) - I_i \right]. \tag{A.20}$$

Meanwhile, for the term $F_{(I,ji)}$, we have

$$\frac{\partial F_{(I,ji)}}{\partial H_i} = \frac{C_I}{k_{ji} H_i^2} \left[I_i \eta_{I,ij} - I_j \eta_{I,ji} + \sum_{k \neq i,j} (I_i \eta_{I,ik} - I_k \eta_{I,ki}) - I_i \right]. \tag{A.21}$$

Because of feasibility, we can only determine the relationship between migration rates and hospital resources in a two-city model. Then, according to the general implicit function theorem, the derivative becomes

$$\frac{\partial \eta_{S,12}}{\partial H_1} = -\frac{\begin{vmatrix} \frac{\partial F_{(S,12)}}{\partial H_1} & \frac{\partial F_{(S,12)}}{\partial \eta_{S,21}} & \frac{\partial F_{(S,12)}}{\partial \eta_{I,12}} & \frac{\partial F_{(S,12)}}{\partial \eta_{I,21}} \\ \frac{\partial F_{(S,21)}}{\partial H_1} & \frac{\partial F_{(S,21)}}{\partial \eta_{S,21}} & \frac{\partial F_{(S,21)}}{\partial \eta_{I,12}} & \frac{\partial F_{(S,21)}}{\partial \eta_{I,21}} \\ \frac{\partial F_{(I,12)}}{\partial H_1} & \frac{\partial F_{(I,12)}}{\partial \eta_{S,21}} & \frac{\partial F_{(I,12)}}{\partial \eta_{I,12}} & \frac{\partial F_{(I,12)}}{\partial \eta_{I,21}} \\ \frac{\partial F_{(I,21)}}{\partial H_1} & \frac{\partial F_{(I,21)}}{\partial \eta_{S,21}} & \frac{\partial F_{(I,21)}}{\partial \eta_{I,12}} & \frac{\partial F_{(I,21)}}{\partial \eta_{I,21}} \end{vmatrix}}{|\boldsymbol{A}|}. \tag{A.22}$$

For other combination of derivatives, they can also derived similarly. We first calculate,

$$\frac{\partial F_{(S,12)}}{\partial H_1} = \frac{\partial F_{(S,21)}}{\partial H_1} = 0, \tag{A.23}$$

$$\frac{\partial F_{(I,12)}}{\partial H_1} = -\frac{C_I}{k_{12}H_1^2}(I_1\eta_{I,12} - I_2\eta_{I,21} - I_1), \tag{A.24}$$

$$\frac{\partial F_{(I,21)}}{\partial H_1} = \frac{C_I}{k_{21}H_1^2}(I_1\eta_{I,12} - I_2\eta_{I,21} - I_1), \tag{A.25}$$

where C_I is shown in (10). Then,

$$\frac{\partial \eta_{S,12}}{\partial H_1} = -\frac{\begin{vmatrix} 0 & 0 & \frac{C_S I_1}{k_{12}}\left(\frac{1}{N_1-D_1}+\frac{1}{N_2-D_2}\right) & -\frac{C_S I_2}{k_{12}}\left(\frac{1}{N_1-D_1}+\frac{1}{N_2-D_2}\right) \\ 0 & 1 & -\frac{C_S I_1}{k_{21}}\left(\frac{1}{N_1-D_1}+\frac{1}{N_2-D_2}\right) & \frac{C_S I_2}{k_{21}}\left(\frac{1}{N_1-D_1}+\frac{1}{N_2-D_2}\right) \\ -\frac{C_I}{k_{12}H_1^2}(I_1\eta_{I,12}-I_2\eta_{I,21}-I_1) & 0 & \frac{C_I I_1}{k_{12}}\left(\frac{1}{H_1}+\frac{1}{H_2}\right)+1 & -\frac{C_I I_2}{k_{12}}\left(\frac{1}{H_1}+\frac{1}{H_2}\right) \\ \frac{C_I}{k_{21}H_1^2}(I_1\eta_{I,12}-I_2\eta_{I,21}-I_1) & 0 & -\frac{C_I I_1}{k_{21}}\left(\frac{1}{H_1}+\frac{1}{H_2}\right) & \frac{C_I I_2}{k_{21}}\left(\frac{1}{H_1}+\frac{1}{H_2}\right)+1 \end{vmatrix}}{\begin{vmatrix} 1 & 0 & \frac{C_S I_1}{k_{12}}\left(\frac{1}{N_1-D_1}+\frac{1}{N_2-D_2}\right) & -\frac{C_S I_2}{k_{12}}\left(\frac{1}{N_1-D_1}+\frac{1}{N_2-D_2}\right) \\ 0 & 1 & -\frac{C_S I_1}{k_{21}}\left(\frac{1}{N_1-D_1}+\frac{1}{N_2-D_2}\right) & \frac{C_S I_2}{k_{21}}\left(\frac{1}{N_1-D_1}+\frac{1}{N_2-D_2}\right) \\ 0 & 0 & \frac{C_I I_1}{k_{12}}\left(\frac{1}{H_1}+\frac{1}{H_2}\right)+1 & -\frac{C_I I_2}{k_{12}}\left(\frac{1}{H_1}+\frac{1}{H_2}\right) \\ 0 & 0 & -\frac{C_I I_1}{k_{21}}\left(\frac{1}{H_1}+\frac{1}{H_2}\right) & \frac{C_I I_2}{k_{21}}\left(\frac{1}{H_1}+\frac{1}{H_2}\right)+1 \end{vmatrix}}. \tag{A.26}$$

For the denominator, we can derive it as

$$\begin{vmatrix} 1 & 0 & \frac{C_S I_1}{k_{12}}\left(\frac{1}{N_1-D_1}+\frac{1}{N_2-D_2}\right) & -\frac{C_S I_2}{k_{12}}\left(\frac{1}{N_1-D_1}+\frac{1}{N_2-D_2}\right) \\ 0 & 1 & -\frac{C_S I_1}{k_{21}}\left(\frac{1}{N_1-D_1}+\frac{1}{N_2-D_2}\right) & \frac{C_S I_2}{k_{21}}\left(\frac{1}{N_1-D_1}+\frac{1}{N_2-D_2}\right) \\ 0 & 0 & \frac{C_I I_1}{k_{12}}\left(\frac{1}{H_1}+\frac{1}{H_2}\right)+1 & -\frac{C_I I_2}{k_{12}}\left(\frac{1}{H_1}+\frac{1}{H_2}\right) \\ 0 & 0 & -\frac{C_I I_1}{k_{21}}\left(\frac{1}{H_1}+\frac{1}{H_2}\right) & \frac{C_I I_2}{k_{21}}\left(\frac{1}{H_1}+\frac{1}{H_2}\right)+1 \end{vmatrix}$$

$$
\begin{aligned}
=&\begin{vmatrix} \frac{C_I I_1}{k_{12}}\left(\frac{1}{H_1}+\frac{1}{H_2}\right)+1 & -\frac{C_I I_2}{k_{12}}\left(\frac{1}{H_1}+\frac{1}{H_2}\right) \\ -\frac{C_I I_1}{k_{21}}\left(\frac{1}{H_1}+\frac{1}{H_2}\right) & \frac{C_I I_2}{k_{21}}\left(\frac{1}{H_1}+\frac{1}{H_2}\right)+1 \end{vmatrix} \\
=&C_I\left(\frac{1}{H_1}+\frac{1}{H_2}\right)\left(\frac{I_1}{k_{12}}+\frac{I_2}{k_{21}}\right)+1. \qquad \text{(A.27)}
\end{aligned}
$$

Meanwhile, for the nominator, we have

$$
\begin{aligned}
&\begin{vmatrix} 0 & 0 & \frac{C_S I_1}{k_{12}}\left(\frac{1}{N_1-D_1}+\frac{1}{N_2-D_2}\right) & -\frac{C_S I_2}{k_{12}}\left(\frac{1}{N_1-D_1}+\frac{1}{N_2-D_2}\right) \\ 0 & 1 & -\frac{C_S I_1}{k_{21}}\left(\frac{1}{N_1-D_1}+\frac{1}{N_2-D_2}\right) & \frac{C_S I_2}{k_{21}}\left(\frac{1}{N_1-D_1}+\frac{1}{N_2-D_2}\right) \\ -\frac{C_I}{k_{12}H_1^2}(I_1\eta_{I,12}-I_2\eta_{I,21}-I_1) & 0 & \frac{C_I I_1}{k_{12}}\left(\frac{1}{H_1}+\frac{1}{H_2}\right)+1 & -\frac{C_I I_2}{k_{12}}\left(\frac{1}{H_1}+\frac{1}{H_2}\right) \\ \frac{C_I}{k_{21}H_1^2}(I_1\eta_{I,12}-I_2\eta_{I,21}-I_1) & 0 & -\frac{C_I I_1}{k_{21}}\left(\frac{1}{H_1}+\frac{1}{H_2}\right) & \frac{C_I I_2}{k_{21}}\left(\frac{1}{H_1}+\frac{1}{H_2}\right)+1 \end{vmatrix} \\
=&-\frac{C_I}{k_{12}H_1^2}(I_1\eta_{I,12}-I_2\eta_{I,21}-I_1)\begin{vmatrix} 0 & \frac{C_S I_1}{k_{12}}\left(\frac{1}{N_1-D_1}+\frac{1}{N_2-D_2}\right) & -\frac{C_S I_2}{k_{12}}\left(\frac{1}{N_1-D_1}+\frac{1}{N_2-D_2}\right) \\ 1 & -\frac{C_S I_1}{k_{21}}\left(\frac{1}{N_1-D_1}+\frac{1}{N_2-D_2}\right) & \frac{C_S I_2}{k_{21}}\left(\frac{1}{N_1-D_1}+\frac{1}{N_2-D_2}\right) \\ 0 & -\frac{C_I I_1}{k_{21}}\left(\frac{1}{H_1}+\frac{1}{H_2}\right) & \frac{C_I I_2}{k_{21}}\left(\frac{1}{H_1}+\frac{1}{H_2}\right)+1 \end{vmatrix} \\
&-\frac{C_I}{k_{21}H_1^2}(I_1\eta_{I,12}-I_2\eta_{I,21}-I_1)\begin{vmatrix} 0 & \frac{C_S I_1}{k_{12}}\left(\frac{1}{N_1-D_1}+\frac{1}{N_2-D_2}\right) & -\frac{C_S I_2}{k_{12}}\left(\frac{1}{N_1-D_1}+\frac{1}{N_2-D_2}\right) \\ 1 & -\frac{C_S I_1}{k_{21}}\left(\frac{1}{N_1-D_1}+\frac{1}{N_2-D_2}\right) & \frac{C_S I_2}{k_{21}}\left(\frac{1}{N_1-D_1}+\frac{1}{N_2-D_2}\right) \\ 0 & \frac{C_I I_1}{k_{12}}\left(\frac{1}{H_1}+\frac{1}{H_2}\right)+1 & -\frac{C_I I_2}{k_{12}}\left(\frac{1}{H_1}+\frac{1}{H_2}\right) \end{vmatrix} \\
=&\frac{C_I C_S I_1}{k_{12}^2 H_1^2}(I_1\eta_{I,12}-I_2\eta_{I,21}-I_1)\left(\frac{1}{N_1-D_1}+\frac{1}{N_2-D_2}\right) \\
&\frac{C_I C_S I_2}{k_{12}k_{21}H_1^2}(I_1\eta_{I,12}-I_2\eta_{I,21}-I_1)\left(\frac{1}{N_1-D_1}+\frac{1}{N_2-D_2}\right) \\
=&\frac{C_I C_S}{k_{12}H_1^2}(I_1\eta_{I,12}-I_2\eta_{I,21}-I_1)\left(\frac{1}{N_1-D_1}+\frac{1}{N_2-D_2}\right)\left(\frac{I_1}{k_{12}}+\frac{I_2}{k_{21}}\right). \qquad \text{(A.28)}
\end{aligned}
$$

Thus,

$$
\frac{\partial \eta_{S,12}}{\partial H_1} = -\frac{\frac{C_I C_S}{k_{12}H_1^2}(I_1\eta_{I,12}-I_2\eta_{I,21}-I_1)\left(\frac{1}{N_1-D_1}+\frac{1}{N_2-D_2}\right)\left(\frac{I_1}{k_{12}}+\frac{I_2}{k_{21}}\right)}{C_I\left(\frac{1}{H_1}+\frac{1}{H_2}\right)\left(\frac{I_1}{k_{12}}+\frac{I_2}{k_{21}}\right)+1} > 0, \qquad \text{(A.29)}
$$

when $I_1\eta_{I,12}-I_2\eta_{I,21}-I_1 < 0$, which is always true since the migration rates should be within the range of 0 to 1.

Similarly, we have the following derivatives.

$$
\frac{\partial \eta_{S,21}}{\partial H_1} = \frac{\frac{C_I C_S}{k_{12}H_1^2}(I_1\eta_{I,12}-I_2\eta_{I,21}-I_1)\left(\frac{1}{N_1-D_1}+\frac{1}{N_2-D_2}\right)\left(\frac{I_1}{k_{12}}+\frac{I_2}{k_{21}}\right)}{C_I\left(\frac{1}{H_1}+\frac{1}{H_2}\right)\left(\frac{I_1}{k_{12}}+\frac{I_2}{k_{21}}\right)+1} < 0 \qquad \text{(A.30)}
$$

$$\frac{\partial \eta_{I,12}}{\partial H_1} = \frac{\frac{C_I}{k_{12}H_1^2}(I_1\eta_{I,12} - I_2\eta_{I,21} - I_1)}{C_I\left(\frac{1}{H_1}+\frac{1}{H_2}\right)\left(\frac{I_1}{k_{12}}+\frac{I_2}{k_{21}}\right)+1} < 0 \tag{A.31}$$

$$\frac{\partial \eta_{I,21}}{\partial H_1} = -\frac{\frac{C_I}{k_{12}H_1^2}(I_1\eta_{I,12} - I_2\eta_{I,21} - I_1)}{C_I\left(\frac{1}{H_1}+\frac{1}{H_2}\right)\left(\frac{I_1}{k_{12}}+\frac{I_2}{k_{21}}\right)+1} > 0 \tag{A.32}$$

In optimal policy, the matrix $\boldsymbol{A}$ becomes

$$|\boldsymbol{A}| = \begin{vmatrix} \boldsymbol{I}_{n(n-1)\times n(n-1)} & \boldsymbol{A}_{(S,ij),(I,kl)} \\ \boldsymbol{A}_{(I,ij),(S,kl)} & \boldsymbol{A}_{(I,ij),(I,kl)} \end{vmatrix}. \tag{A.33}$$

Then, the calculation will be fairly complicated, and will be difficult to judge whether the derivatives are positive or negative.

□

In this proposition, it is stated that susceptible agents will be more inclined to live outside of city 1, without concluding that they will be more inclined to live in city 2. This is because this simplified two-city model leads to the result that susceptible agents prefer to live in the city with fewer hospital resources, and thus the model is not good enough to describe the migration behavior in a pandemic. This unreasonable conclusion is due to the fact that agents only have two alternatives: either living in city 1 or in city 2. To obtain more realistic results, we turn to discuss a model with more cities through numerical analysis in Section 4 in the main text.

Appendix E Components of Different Types of Agents in Each City

In this section, we show the components of different types of agents in each city in the following situations: the initial state, the final state in laissez-faire equilibrium, and the final state in optimal policy. We only consider the case when there are three cities: an epidemic focus, a big city, and a small city. The hospital resources in these three cities are allocated as 1,000, 3,000, and 100, respectively. The pie graphs are shown in Figure A.1.

From these pie graphs, we can see that the infected agents are more concentrated in city 1 in optimal policy than in laissez-faire equilibrium, and the aggregate ratio of infected agents in laissez-faire equilibrium is larger than that in optimal policy. These observations are consistent with our analysis in Section 4.4.

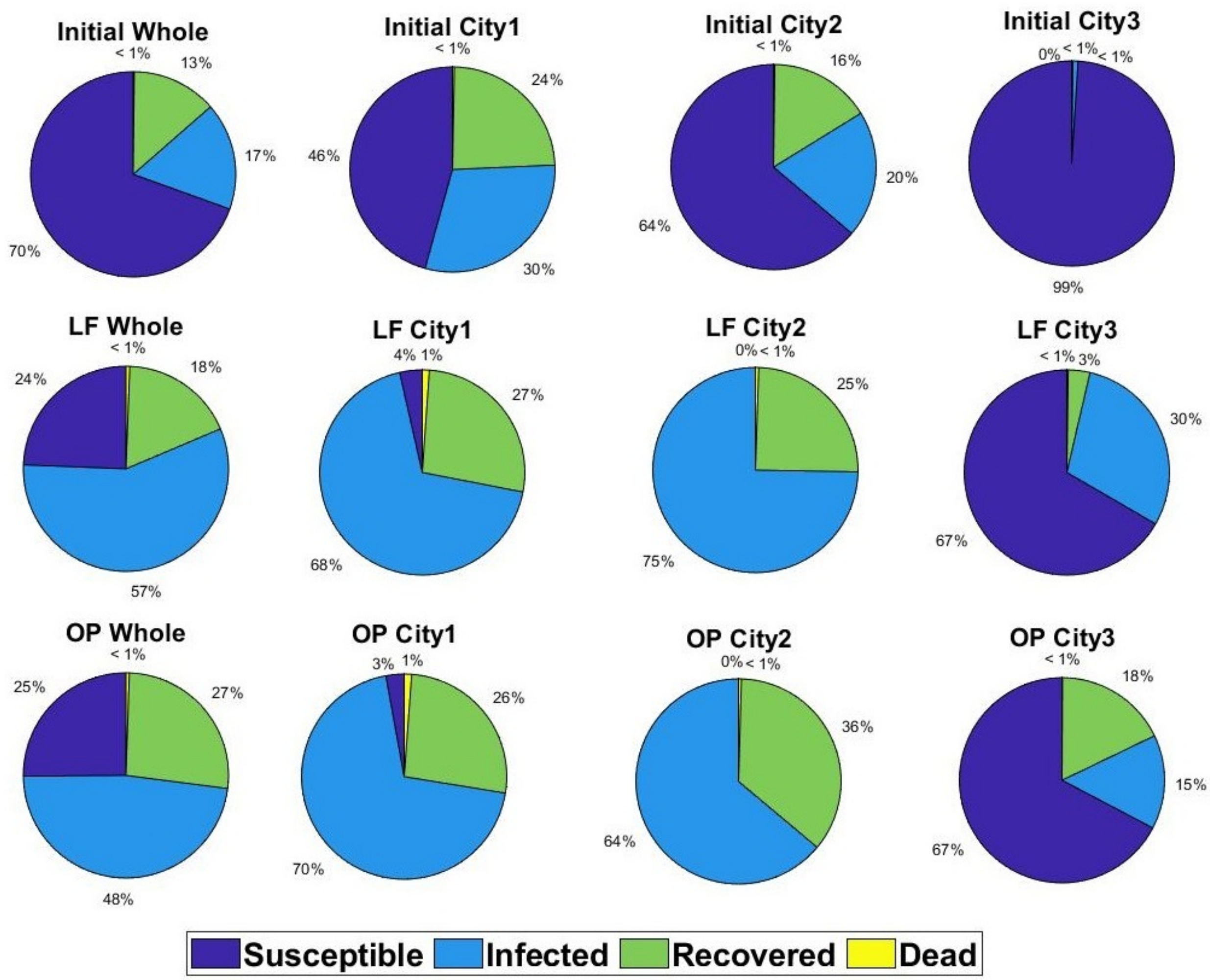

Figure A.1: Components of Different Types of Agents in Each City

Notes. The initial states of all the three cities are defined the same as those in Figure 2.